Bohnhoff, M., Rische, M., Meier, T., Becker, D., Stavrakakis, G., Harjes, H.-P. (2006): Microseismic activity in the Hellenic Volcanic Arc, Greece, with emphasis on the seismotectonic setting of the Santorini–Amorgos zone. - Tectonophysics, 423, 1-4, 17-33,

DOI: 10.1016/j.tecto.2006.03.024.

Available online at www.sciencedirect.com
SCIENCE DIRECT
ELSEVIER
TECTONOPHYSICS
Tectonophysics xx (2006) xxx – xxx
www.elsevier.com/locate/tecto

Microseismic activity in the Hellenic Volcanic Arc, Greece, with emphasis on the seismotectonic setting of the Santorini–Amorgos zone

Marco Bohnhoff [a,*], Martina Rische [b], Thomas Meier [b], Dirk Becker [b], George Stavrakakis [c], Hans-Peter Harjes [b]

[a] *GeoForschungsZentrum, Telegrafenberg D424, 14473 Potsdam, Germany*
[b] *Department of Geosciences, Ruhr-University Bochum, Germany*
[c] *National Observatory of Athens, Institute of Geodynamics, Greece*

Received 16 March 2005; received in revised form 23 September 2005; accepted 25 March 2006

Abstract

The volcanic arc of the Hellenic subduction zone with its four volcanic centers is of major relevance when evaluating the seismovolcanic hazard for the Aegean region. We present results from a 22-station temporary seismic network (CYCNET) in the central Hellenic Volcanic Arc (HVA). CYCNET recordings allow to analyze the level and spatio-temporal evolution of microseismic activity in this region for the first time. A total of 2175 events recorded between September 2002 and July 2004 are analyzed using statistical methods, cluster analysis and relative relocation techniques. We identify distinct regions with significantly varying spatio-temporal behavior of microseismicity. A large portion of the seismic activity within the upper crust is associated with the presence of islands representing horst structures that were generated during the major Oligocene extensional phase. In contrast, the central part of the Cyclades metamorphic core complex remains aseismic considering our magnitude threshold of 1.8 except one spot where events occur swarm-like and with highly similar waveforms.

The highest activity in the study area was identified along the SW–NE striking Santorini–Amorgos zone. Within this zone the submarine Columbo volcano exhibits strong temporal variations of seismic activity on a high background level. This activity is interpreted to be directly linked to the magma reservoir and therein the migration of magma and fluids towards the surface. NE of Columbo where no volcanic activity has yet been reported we observe a similar seismicity pattern with small-scaled activity spots that might represent local pathways of upward migrating fluids or even developing volcanic activity within this zone of crustal weakness. In contrast, the Santorini and Milos volcanic complexes do not ~~shot~~ show significant temporal variations and low to moderate background activity, respectively. Relating our results to the distribution of historical earthquakes and the GPS-derived horizontal velocity field we conclude that the Santorini–Amorgos zone is presently in the state of right-lateral transtension reflecting a major structural boundary of the volcanic arc subdividing it into a seismically and volcanically quiet western and an active eastern part.

Keywords: Seismology; Seismotectonic; Hellenic subduction zone; Hellenic Volcanic Arc; Temporary networks

1. Tectonic setting

The Hellenic subduction zone represents the seismically most active region in Europe with predominant

* Corresponding author. Tel.: +49 331 2881327; fax: +49 331 2881328.
E-mail address: bohnhoff@gfz-potsdam.de (M. Bohnhoff).

0040-1951/$ - see front matter © 2006 Published by Elsevier B.V.
doi:10.1016/j.tecto.2006.03.024

activity along the Hellenic arc (Fig. 1a). The convergent plate boundary between the African lithosphere and the Aegean domain as part of the Eurasian plate is located 100–150 km south of the Hellenic arc in the Libyan Sea and approaches the passive continental margin of northern Africa due to roll back of the Hellenic subduction zone and the convergence between Africa and Eurasia (e.g. Le Pichon and Angelier, 1979; Jackson and McKenzie, 1988; Le Pichon et al., 1995; Meier et al., 2004). The overall rate of convergence is about 4 cm/a (e.g. Mc Kenzie, 1970; Jackson, 1994; Le Pichon et al., 1995; Mc Clusky et al., 2000) with a major contribution from the >3 cm/a SW-ward migration of the southern Aegean domain. A well-developed Benioff zone was identified by seismological observations to a depth of 150–180 km below the central Aegean (Galanopoulos, 1963; Papazachos, 1973; Makropoulos and Burton, 1981; Papadopoulos et al., 1986; Papazachos et al., 2000). The volcanic arc of the Hellenic subduction zone (Hellenic Volcanic Arc, referred to as HVA in the following) is located about 150 km to the north of the Hellenic arc in the southern Aegean Sea. The HVA follows the four main volcanic centers of the Hellenic subduction zone namely Aegina, Milos, Santorini and Nisyros from West to East. In this paper, we focus on the central HVA represented by the Cyclades island group (see Fig. 1a). The Cyclades are assumed to represent a classical example of a high-pressure belt in a back-arc environment (Trotet et al., 2001). Major zones of extensional detachments were described of which some have been shown to be related to post-orogenic crustal-scale extension (e.g. Lister et al., 1984; Avigad and Garfunkel, 1989; Gautier et al., 1993; Gautier and Brun, 1994). There is general agreement on a two-stage extension of the Aegean domain since Oligocene times (e.g. Tirel et al., 2004 and references therein). The first phase of extension occurred during Oligocene to middle Miocene and was initiated by the southward migration of the subducting African lithosphere. This dominantly NS-stretching period was marked by the formation of core complexes in the Cyclades that today form the central HVA (see also Le Pichon and Angelier, 1979; Lister et al., 1984). However, extension was accompanied or possibly alternated with shortening perpendicular to the stretching direction recognized in large-scale NE–SW to NNE–SSW trending features (Avigad et al., 2001) one of which is the Santorini–Amorgos zone of crustal weakness (see Fig. 1b). The second phase of extension which occurred in Late Miocene is related either to the westward extrusion of Anatolia or to gravity spreading of the Aegean lithosphere (see discussion in Gautier et al., 1999). During this phase, the Cyclades block remained rather inactive and stretching was concentrated in the North Aegean and in the Cretan Sea (see also Walcott and White, 1998).

Volcanic activity in the HVA began approximately 3–4 Ma ago and the area is considered as a region of extensive Quaternary volcanism (e.g. Keller et al., 1990). The main explosive centers of the Upper Quaternary are Milos, Santorini and Nisyros. The volcanic island of Milos has been the site of explosive rhyolitic volcanism during Plio-Quaternary times (Rinaldi and Campos Vinuti, 2003) and no volcanic activity was reported for the last 40 ka. A comprehensive summary on the eruption history of the Santorini volcano complex was given by Druitt et al. (1999) and Friedrich (2000). Activity of the Santorini complex started ~ 600 ka b.p. (Perissoratis, 1995) and the volcano is well known for its Late Bronze Age eruption of 1640 BC that was classified as very large (Volcanic Explosivity Index 6.9 or 7.0; Dominey-Howes, 2004). This eruption also formed the general shape of the present caldera. Historic activity has resulted in the present-day islands of Palea and Nea Kameni. Approximately 7 km NE of the main island of Santorini, a new volcanic center broke the water surface in 1650 AD (e.g. Vougioukalakis et al., 1994; Perissoratis, 1995). This volcanic field is referred to as the Columbo volcanic reef and is considered to be active today (Dominey-Howes and Minos-Minopoulos, 2004).

2. Seismicity in the HVA

Seismicity in the south Aegean region predominantly follows the Hellenic arc as identified in the relocated ISC catalogue by Engdahl et al. (1998) that covers the time period 1964–1998 and is complete to $M=4$ (Fig. 1a). In

Fig. 1. (a) Main tectonic elements of the south Aegean region and GPS-derived horizontal velocity field (simplified, after Mc Clusky et al., 2000). Triangles represent the volcanic centers of Aegina, Milos, Santorini and Nisyros (from west to east). Circles are hypocenters from the relocated ISC catalogue (Engdahl et al., 1998) for the time interval 1964–1998 (complete for $M>4$). The Cyclades region is marked by the rectangle and enlarged in (b). Hypocentral depth scales with shading and magnitude scales with size of circles. The bold line indicates the active continental margin (after e.g. Bohnhoff et al., 2001; Brönner, 2003). Arrows indicate the left-lateral transtensional system consisting of the Ptolemeus, Pliny and Strabo deep sea depressions (from West to East). (b) Distribution of hypocenters in the central Hellenic Volcanic Arc (HVA) during the period 1950–2004 as recorded by the permanent Greek network that is operated by the National Observatory of Athens (NOA). The catalog is complete for $M>3$. Hypocentral depth scales with shading and magnitude scales with size of circles (encoding different than in (a)). The ellipse marks the Santorini–Amorgos area and the black squares mark the two $M>7$ events of 1956 (Papadopoulos and Pavlides, 1992).

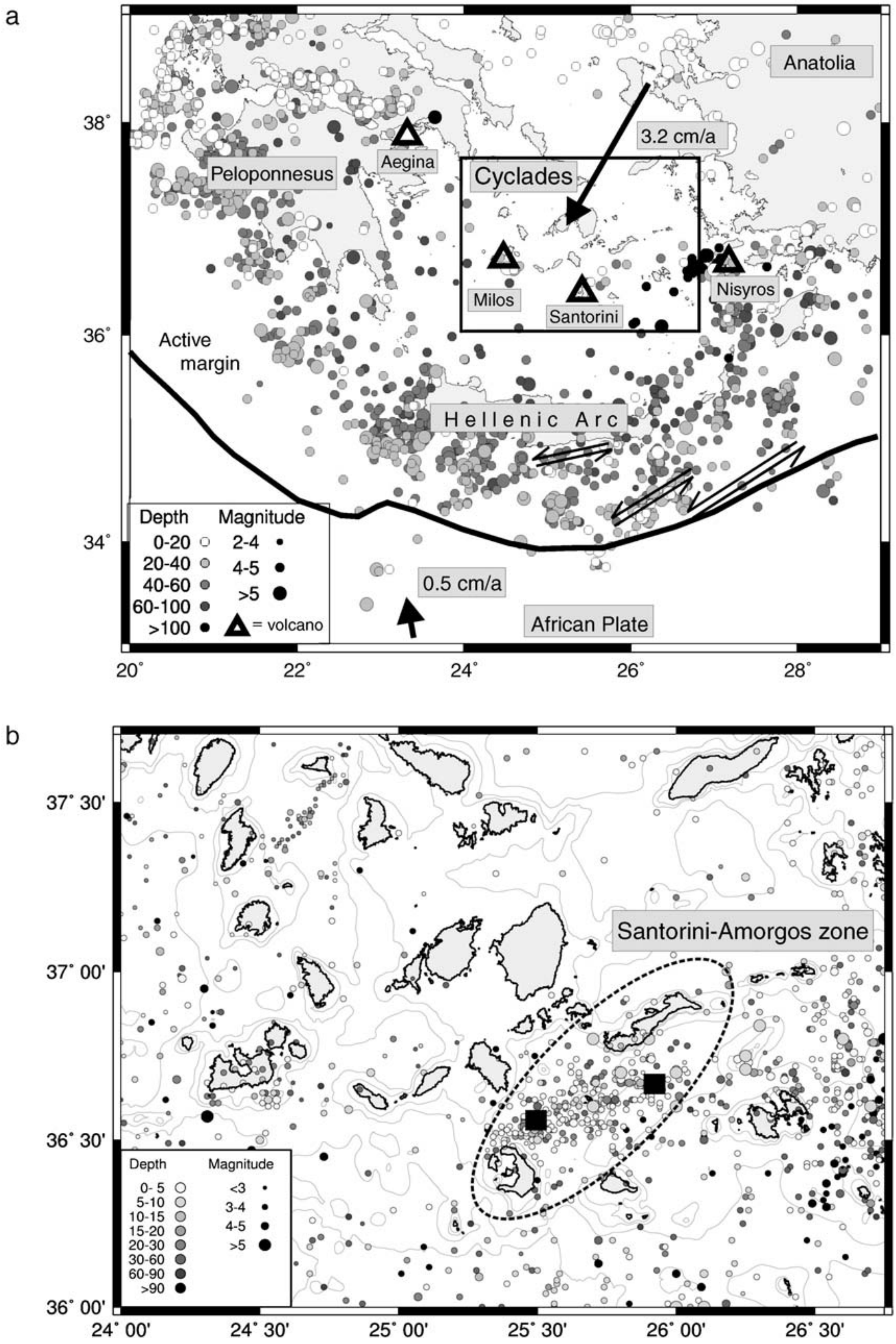
a
Anatolia
3.2 cm/a
Aegina
Peloponnesus
Cyclades
Milos
Santorini
Nisyros
Active margin
Hellenic Arc
Depth
Magnitude
0-20
20-40
40-60
60-100
>100
2-4
4-5
>5
= volcano
0.5 cm/a
African Plate
38°
36°
34°
20°
22°
24°
26°
28°
b
Santorini-Amorgos zone
Depth
Magnitude
0- 5
5-10
10-15
15-20
20-30
30-60
60-90
>90
<3
3-4
4-5
>5
37° 30'
37° 00'
36° 30'
36° 00'
24° 00'
24° 30'
25° 00'
25° 30'
26° 00'
26° 30'

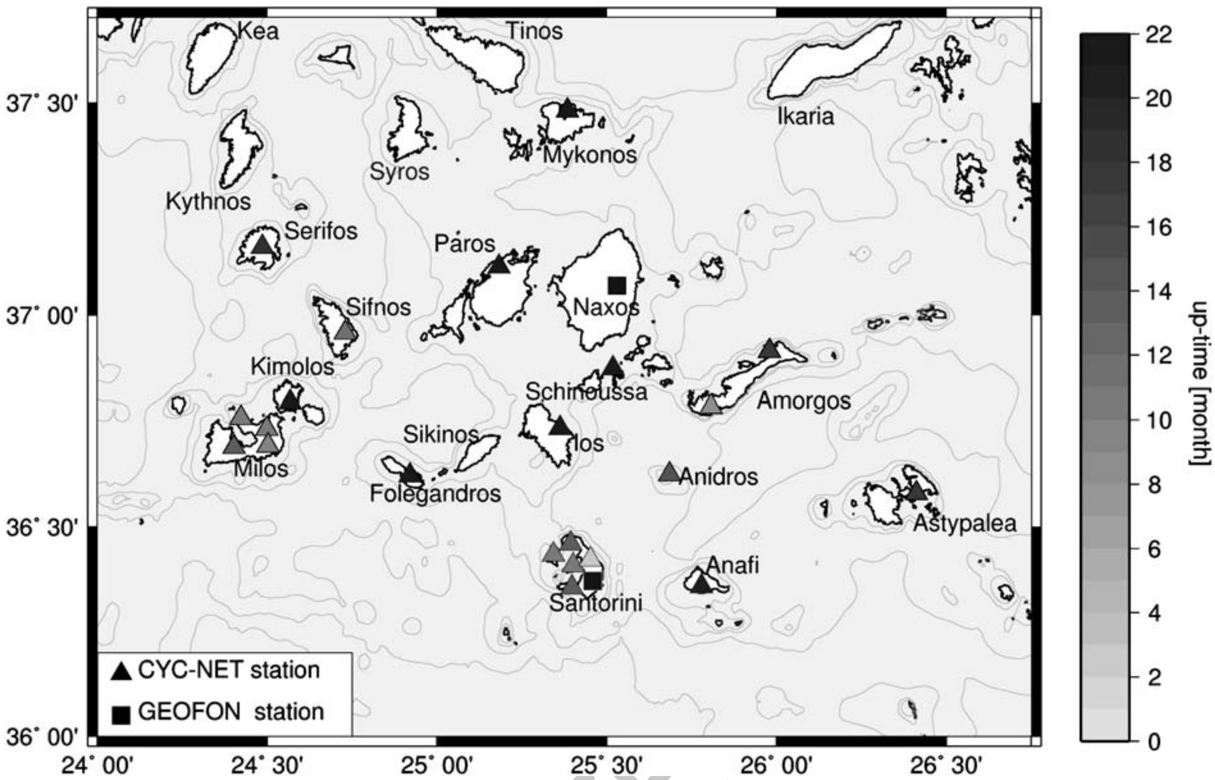

Fig. 2. Station distribution of the Cyclades temporary seismological network (CYCNET) that is operated in the central Hellenic Volcanic Arc since autumn 2002 (Bohnhoff et al., 2004). Triangles mark newly deployed stations of CYCNET and their shading represents individual uptime (scaled to the maximum of 22 months (September 2002–July 2004). Black squares represent stations of the permanent global GEOFON network (Hanka and Kind, 1994). Thin lines mark the 100, 200 and 500 m isolines of water depth, respectively.

general, activity at the HVA is smaller compared to the forearc region and concentrated at the volcanic centers and along the SW–NE trending Santorini–Amorgos zone of crustal weakness. On average, hypocentral depth increases towards the NNE reflecting the subducting oceanic African lithosphere. The catalogue for the central HVA based on recordings from the permanent Greek seismic network that is operated by the National Observatory of Athens (NOA) is complete to $M=3$ and covers the time span 1950–2004 (Fig. 1b). There, the distribution of hypocenters indicates an increasing activity from West to East and the dominantly active regions around Milos and between Santorini and Amorgos are confirmed. Interestingly, the inner part of the metamorphic core complex around the islands of Paros and Naxos appears aseismic also for this magnitude level and a diffuse distribution of hypocenters is observed for the remaining parts of the central HVA. Most events of the NOA-catalogue are located within the crust and only a small number is associated with the Benioff zone at 100–150 km depth.

The two largest earthquakes in the entire south Aegean region during the last century occurred in 1956 within only 13 min and had magnitudes of $M_s=7.4$ and 7.2, respectively. Both events were located between Santorini and Amorgos (indicated by rectangles in Fig. 1b) and they were followed by at least 20 aftershocks of $M>4$ within five months (Papadopoulos and Pavlides, 1992; Papazachos et al., 2000). Interestingly, the hypocenters of this seismic sequence form the same SW–NE trend between Santorini and Amorgos that is observed from instrumental seismicity from the ISC and NOA catalogues. Based on the presently available data, the most challenging objective towards a better understanding of the present

Table 1
Velocity model for the central HVA based on a wide-aperture seismic line in the eastern HVA (Makris and Chonia, 1999), results of receiver-function analysis of CYCNET data (Endrun et al., 2005; Endrun et al., pers. comm.) and inversion of gravity data (Tirel et al., 2004)

V_p [km/s]	z [km]
5.00	0.00
5.50	2.00
5.80	5.00
6.70	12.00
7.90	24.00

See text for details.

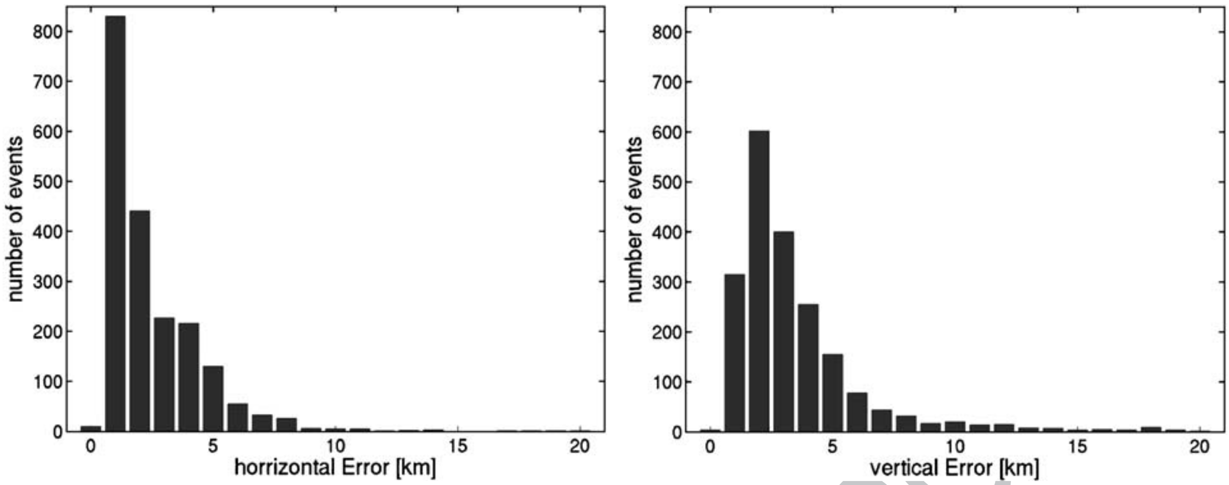

Fig. 3. Distribution of horizontal (~~ERH,~~ left) and vertical (~~ERZ,~~ right) location errors for the entire CYCNET catalogue containing 2175 events. The majority of events have errors ≤ 3 km. Errors were determined using the HYP71 routine (Lee and Lahr, 1972, 1975). See text for details.

seismotectonic setting of the HVA is to improve the location accuracy and to lower the magnitude-detection threshold for local seismic activity in this region. Local temporary networks were operated on Santorini (Panagiotopoulos et al., 1996) and on Milos (Ochmann et al., 1989) for several months. Data from these deployments allowed to identify a strong spatio-temporal clustering below Milos where time intervals with average seismic activity of 3–5 events per day were interrupted by single days with up to 600 events. The events were weak ($M \sim 2$) and occurred within the uppermost 10 km. No such temporal clustering was observed at the Santorini volcano where seismic activity was low and concentrated to the NE of the caldera.

A regional temporary network was installed in the south Aegean in 1988 (Hatzfeld et al., 1993) that covered also the central HVA. However, only about ten events were recorded in the Cyclades region and it was concluded that seismicity in this region is sparse. In this paper we focus on microseismic activity in the central HVA based on recordings from a temporal seismic network in the Cyclades island group (CYCNET). CYCNET allows to monitor the entire central HVA at low magnitude-detection threshold using digital data acquisition technology for the first time. We analyze the spatio-temporal behavior of seismic activity using statistical methods as well as cluster analysis and relative relocation techniques and focus on the role of the Santorini–Amorgos zone for the seismotectonic setting of this region.

3. Data base

With the aim to simultaneously monitor the microseismic activity in the central HVA we installed a seismic network on the Cyclades island group (CYCNET) in autumn 2002 (Bohnhoff et al., 2004). For common onshore networks the distribution of stations is restricted mainly by the level of civilian noise, ground coupling and station access. In contrast, the selection of recording sites for a seismic network in the area of consideration is primarily restricted by the distribution of adequately located islands of sufficient size. Our final deployment included 22 stations on 17 islands covering the entire central HVA. Fig. 2 shows the distribution of CYCNET stations where the uptime of each recording unit is indicated by the shading of the station symbol. Most islands are equipped with a single seismic station. At the

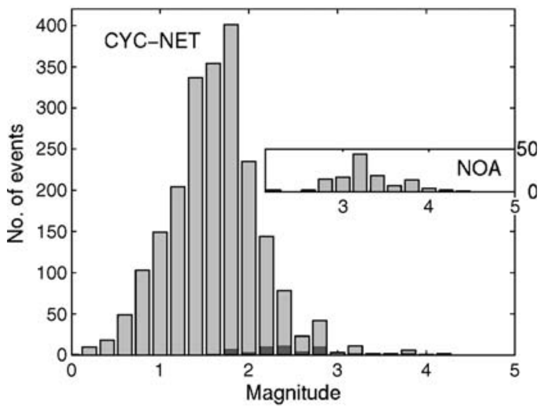

Fig. 4. Magnitude-frequency distribution for the CYCNET catalogue containing all 2175 events within 24.0–26.75°E and 36.0–37.7°N with no depth limitation covering the time interval September 2002–July 2004. Dark gray bars indicate the 51 events located at >60 km depth. The inset shows the magnitude frequency distribution of the NOA catalogue for the same area and time interval (127 events).

volcanic centers of Milos and Santorini station spacing is denser to further decrease the detection threshold. In addition, two stations of the GEOFON network (Hanka and Kind, 1994) enlarge the CYC-NET. Our particular note among the CYC-NET is the station on Anidros, a small (2 km^2) uninhabited island between Santorini and Amorgos that cannot be reached by regular traffic. Because of the strong seismic activity in this region (see Fig. 1b) this station improves location accuracy significantly. Considering the two arrays on Milos and Santorini as one station results in a mean station-spacing of 40 km for CYCNET. All stations are equipped with the same data-logger (Earth Data PR6-24-3AA portable field recorder; Earth Data Ltd., 2002). 16 of the 22 stations are equipped with short-period sensors (type MARK 4L-3C, eigenfrequency 1 Hz). The remaining six stations are equipped with broad-band seismometers (STS-2). Data are continuously sampled at 100 samples per second on three components and the quality of recordings achieved by CYCNET is comparable to those from larger islands such as Crete and thus unexpectedly high (see Bohnhoff et al., 2004, for details).

In this study we consider the time interval September 2002–July 2004. To evaluate the data, we ran a STA/LTA (short-term average/long-term average) trigger on the vertical component of each station as a first step. Events were selected if passing a coincidence trigger (>3 stations) combined with an algorithm neglecting events far outside CYCNET. This was done to exclude the strong seismic activity along the Hellenic arc and in the Nisyros region from further consideration. Onsets of P and S phases were picked manually. A total of 45885 (P) and 39646 (S) onsets were identified, respectively, and served as input together with S–P times if available. To determine the hypocenters we applied the HYPO71 routine (Lee and Lahr, 1972, 1975) that includes a linearized hypocenter inversion. The 1D-velocity model that we used to locate earthquakes is shown in Table 1. The shallower part of the model was taken from results of a wide-aperture seismic profile in the eastern HVA around Nisyros (Makris and Chonia, 1999) as no published data on the shallower velocity structure in the central HVA exist so far. However, we assume that the structure along the volcanic arc does not differ significantly and thus does not affect the location accuracy. The deeper part of the model was calculated from CYCNET recordings using receiver-function analysis techniques (Endrun et al., 2005; Endrun et al., pers. comm.) which basically confirms a Moho depth of 24 km in this area as derived from gravity modeling (Tirel et al., 2004). Furthermore, linearised inversion of Rayleigh-wave dispersion curves with CYCNET data leads to a 1D-velocity model for S-waves (Endrun et al., pers. comm.) and allowed to calculate P-wave velocities for the single layers of our model assuming a v_p/v_s ratio of 1.8.

As the hypocentral depth is sensitive to the start location we iteratively varied this parameter between 5 and 40 km and proceeded with the solution resulting in the lowest root mean square (RMS) value. With this we were able to locate a total of 3438 events. The hypocenter catalogue was then restricted to the range 24.0–26.75°E and 36.0–37.7°N with no depth limitation and only events based on at least eight (including at least two S) picks and a RMS value <0.7 s were considered for further analysis. This resulted in a final hypocenter catalogue containing 2175 events. Fig. 3 shows the horizontal and vertical errors for the entire catalogue of 2175 events used for further evaluation, respectively. The majority of events have errors ≤ 3 km which is clearly sufficient taking into consideration the average station spacing of 40 km for CYCNET. Fig. 4 shows the magnitude-frequency distribution for the CYCNET catalogue. The threshold of completeness is $M \sim 1.8$ and the largest event had a magnitude of 4.2. Events located at depths >60 km are separately indicated by the dark grey bars. For reference we also plotted the NOA catalogue for the same time interval in Fig. 4. The significant difference between both catalogues exemplifies the benefit of densely spaced temporary seismic networks to evaluate the level of microseismic activity in regions classified as aseismic based on existing hypocenter catalogues.

The spatial distribution of hypocenters recorded by CYCNET is plotted in Fig. 5 in map view. The hypocentral depth is color-encoded and grey-shading in the background indicates water depth. More then 80% of the events occur within the uppermost 15 km, i.e. within the Aegean crust that has an average crustal thickness of ~ 24 km in this region (Tirel et al., 2004). Furthermore, a significant number of events is located at intermediate depth levels and can thus be associated with the Benioff zone at 100–150 km depth. These events were located incorporating recordings from surrounding permanent NOA stations to enlarge CYCNET's aperture which significantly improved the accuracy of hypocenter determination. Apart from crustal and intermediate-depth seismicity, a small number of earthquakes are observed at 24–60 km depth. These events might be associated with rising fluids and magma below the volcanic centers of the central HVA. In this study we focus on the seismic activity within the upper plate and thus do not further consider earthquakes below the Moho.

4. Discussion

4.1. Spatio-temporal microseismic pattern in the central HVA

Shallow seismicity in the central HVA does not occur randomly distributed but, in contrast, shows a number of systematic spatio-temporal patterns. A clear spatial clustering is observed from the distribution of hypocenters in Fig. 5. A large portion of the seismic events is related to the occurrence of islands and adjacent offshore areas of < 100 m water depth. This effect is not an artifact of CYCNET's station distribution as it is observed also on islands where no seismic station was operated (e.g. islands of Sikinos and Syros) and even on islands outside the network (e.g. Kythnos, Kea, Tinos and Ikaria) (see Figs. 2, 5). In contrast, most offshore regions exhibit a significantly lower level of seismic activity, e.g. between Paros and Mykonos, or do not contain a single event at all like the region between Paros and Folegandros. The region surrounded by the chain of islands consisting of Ios–Folegandros–Milos–Serifos–Syros–Mykonos is seismically almost inactive except for the spot between Paros and Naxos that will be discussed in more detail later in the text. Interestingly, the area of low activity coincides with the inner part of the metamorphic core complex that formed during the Oligocene major extensional phase (e.g. Lister et al., 1984; Trotet et al., 2001) and that today represents a major part of the Cyclades island group. Apart from the relation between seismic activity and the occurrence of islands a large number of events align along the SW–NE trending Santorini–Amorgos zone. Here, we observe also the highest activity in the entire study area that clusters at two spots ~ 5–10 km NE of Santorini and

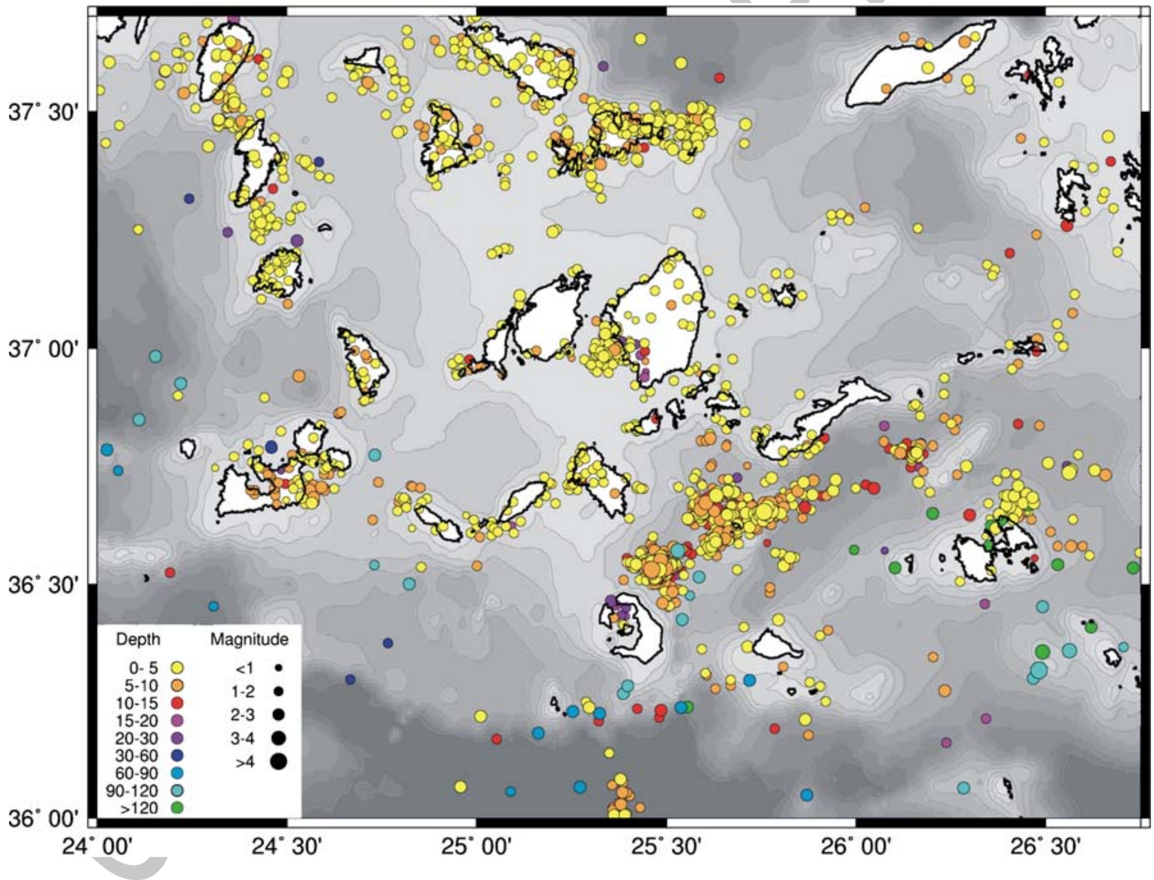

Fig. 5. Hypocenter catalogue for the central Hellenic Volcanic Arc determined by CYCNET during the time interval September 2002–July 2004. The shown catalogue includes all 2175 events that were selected for further interpretation (see text for details). Hypocentral depth is color encoded and size of circles scales with magnitude. Gray shading indicates water depth in 100 m steps for the first 500 m; dark gray areas in the south reach water depth of more than 1000 m. Shallow seismicity in the central HVA does not occur randomly distributed but shows a number of systematic spatio-temporal patterns. A large portion of the seismic events is related to the occurrence of islands and adjacent offshore areas of < 100 m water depth. This effect is not an artifact of CYCNET's station distribution as it is observed also on islands where no seismic station was operated and even on islands outside the network. In contrast, most offshore regions exhibit a significantly lower level of seismic activity.

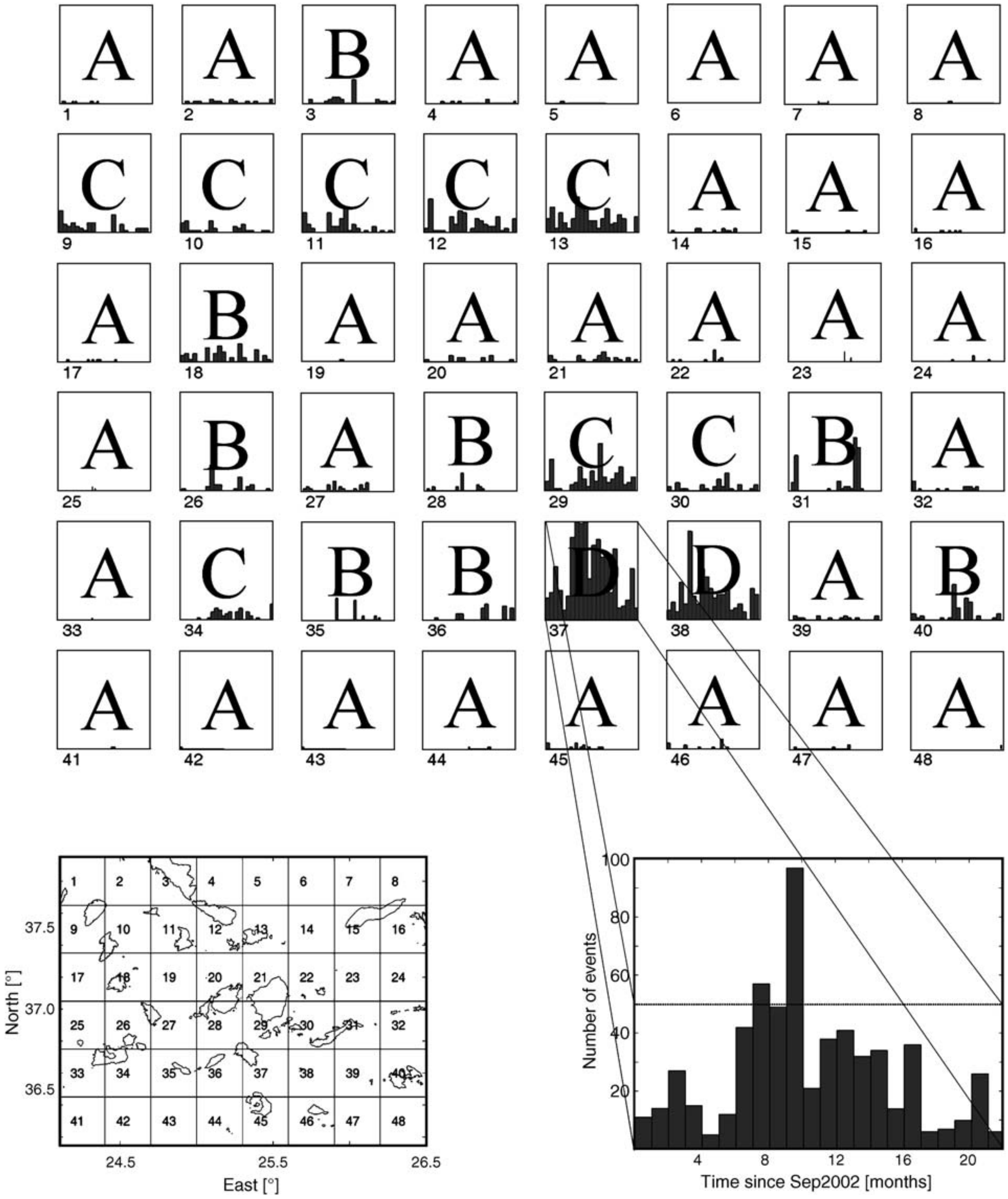

Fig. 6. Spatio-temporal evolution of seismicity within a total of 48 boxes (size: Δlat = 0.3° and Δlon = 0.3° limited to a hypocentral depth of 24 km) covering the central Hellenic Volcanic Arc. The event rate is scaled to 50 to visualize the locally varying activity pattern. Four different types (A–D) of activity pattern are identified and plotted onto the boxes (see text for details). In box 37, activity exceeds the monthly event rate of 50 during two months; it is therefore enlarged scaled to the overall maximum of 100 exemplifying the overall highest seismic activity that is directly linked to the here located submarine Columbo volcano. In the lower left we plotted a map view of all 48 boxes.

around Anidros (see Fig. 5). This zone was also identified as the most active region within the central HVA from the ISC and NOA catalogues (Fig. 1). Note, that the here presented catalogue contains magnitudes < 3 with a few exceptions only and thus covers a different rupture length.

To further analyze the occurrence of microseismic activity and to elucidate its spatio-temporal evolution we subdivided the central HVA into 48 boxes with an equal size of 0.3° × 0.3° restricted to the uppermost 24 km (see Fig. 6). Within each of the 48 boxes we compute the temporal evolution of seismic activity in terms of monthly event rate. The results allow to identify four different types of spatio-temporal behavior in the area of investigation referred to as type A–D in the following. Type A is characterized by little or almost no seismic activity during the entire observation period. This type is observed in a total of 30 boxes and thus represents almost 65% of the central HVA. To a large extend, these boxes are located at the outer part of CYCNET. However, this is not only an artifact of the network geometry as a number of aseismic boxes are located also within the network (e.g. 19–22, 27). Type B seismicity represents a low background level interrupted by short-term peaks of high activity. Such behavior is observed in boxes 3, 26, 28, 31, 35, 36 and 40. Type B seismicity is a possible indicator for swarm activity and may contain earthquake cluster, i.e. events with highly similar waveforms. However, we cannot exclude that boxes considered as type A might host type-B activity with periods of silence being at least as long as our observation period. Type-C activity reflects boxes with considerable background activity without significant variations during the recording period. This is observed along a west–east trend in boxes 9–13 following the

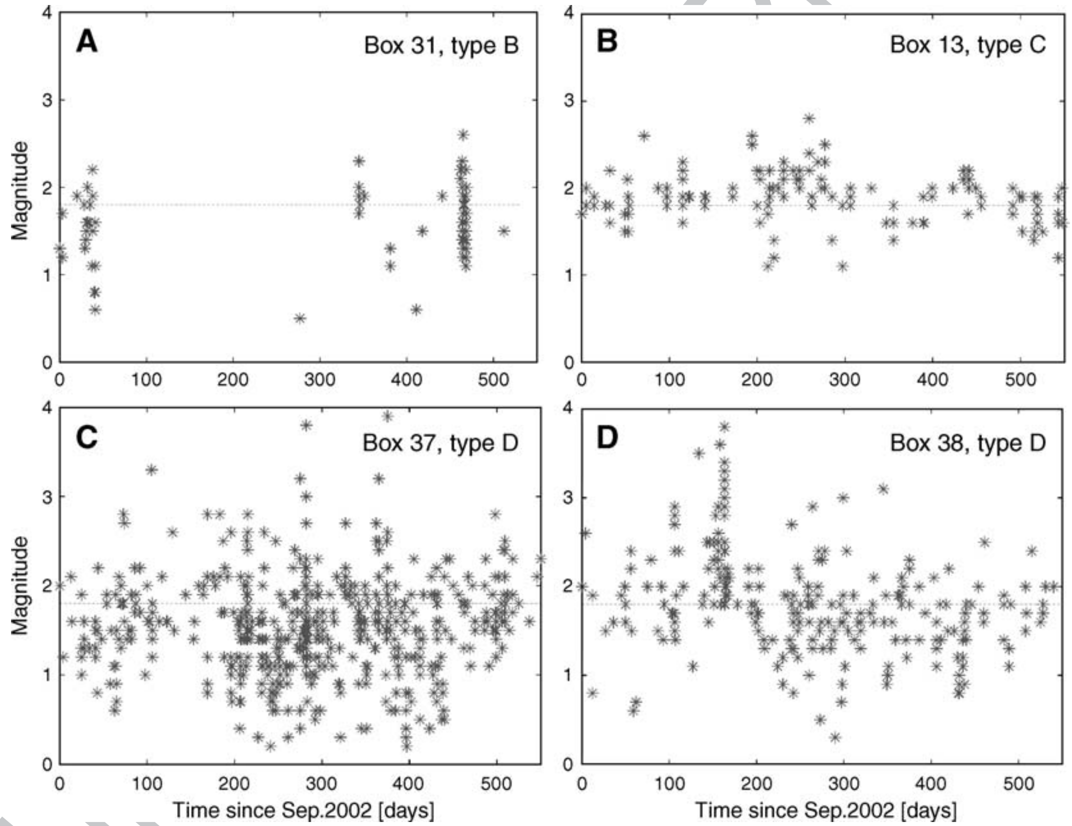

Fig. 7. Temporal distribution of magnitudes within four boxes that are representative for the different types of spatio-temporal seismicity pattern observed in the central Hellenic Volcanic Arc. The dotted line indicates the overall magnitude threshold for CYCNET (1.8). (A) Seismicity SE of Amorgos (box 31) shows strong temporal clustering that covers two orders of magnitude. Two main and one weaker peaks of activity are identified of which the latest is also the strongest and active for ~ 7 days. In between, we observe a >1 year long period of seismic quiescence. This pattern indicates seismic swarm activity. (B) Seismic activity on and around Mykonos (box 13) is restricted to magnitudes 2 ± 0.5 to a large extent. (C and D) The area NE of Santorini hosts the highest in the area of investigation (boxes 37 and 38). The distribution of magnitudes reflects the long-period change of activity within both boxes and clearly indicates the absence of mainshock–aftershock behavior although the magnitude range is high. The activity within box 37 reflects the today-active Columbo volcanic reef located ~ 5–10 km NE of Santorini. The area around Anidros (box 38) shows a similar activity pattern as Columbo, however, no volcanic activity has yet been reported for this part of the Santorini–Amorgos zone.

occurrence of islands in this part. In addition, type-C activity is identified in boxes 18, 29, 30 and 34. Finally, activity of type D is described by an overall strong seismic activity with significant temporal variations. This is observed in boxes 37 and 38, i.e. between Santorini and Amorgos around the submarine Colombo volcano and the island of Anidros. The monthly event rate in Fig. 6 is uniformly scaled to 50 for all 48 boxes for visualization reasons. Only activity in box 37 (area around Columbo) exceeds this rate during two months and is therefore shown enlarged and complete in the lower right of Fig. 6.

In the following we discuss representative examples for the different types of activity in more detail which are boxes 31 (type B), 13 (type C) and 37+38 (type D). Fig. 7 shows the temporal evolution of event magnitudes for these four boxes. Seismicity SE of Amorgos (box 31, Fig. 7A) shows strong temporal clustering at a single location that covers two orders of magnitude (see also hypocentral distribution in Fig. 5). Two main and one weaker peaks of activity are identified of which the latest is also the strongest and active for ~ 7 days. In between, we observe a > 1 year long period of seismic quiescence. This pattern indicates seismic swarm

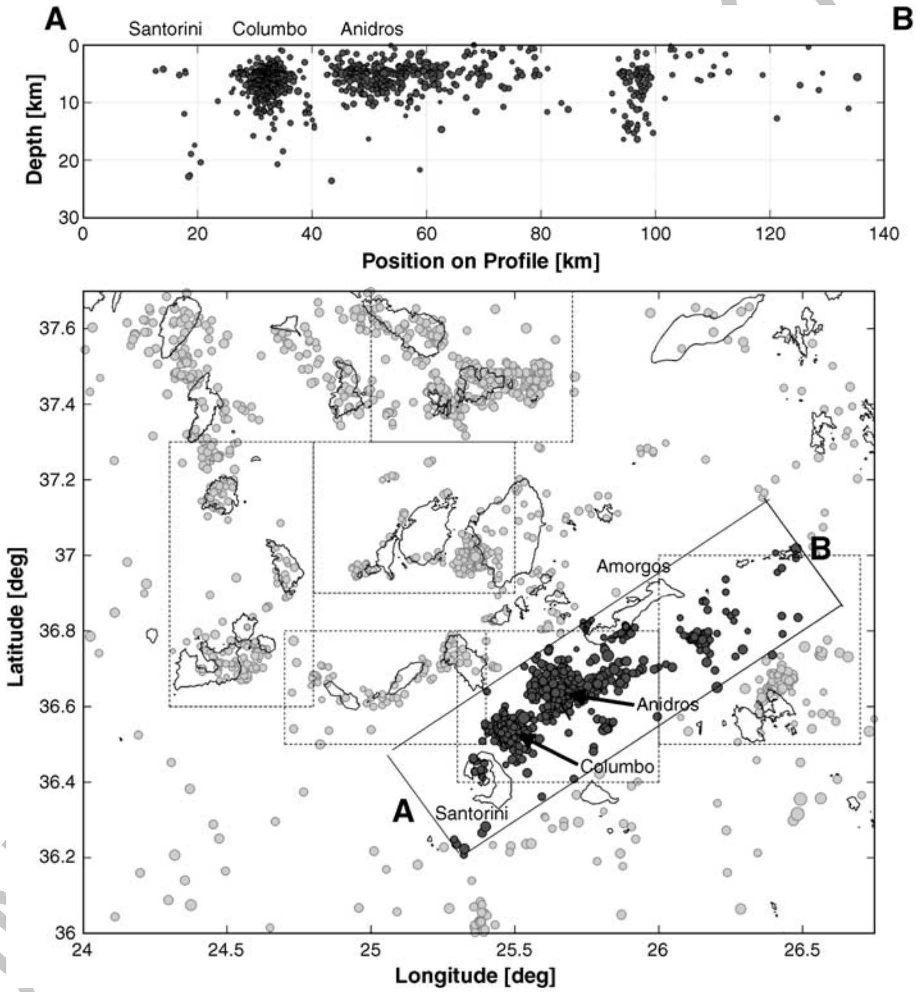

Fig. 8. Seismic activity in the Santorini–Amorgos zone observed by CYCNET. The upper part shows a depth section that includes all events within a 40 km wide SW–NE trending profile that is indicated in the lower part by the ~ N50°E trending rectangle. A total of 1038 events are included in this profile which is almost half of the entire CYCNET data base. The distribution of events along the profile suggests that the activity just NE of Santorini is related to the volcanic activity of Mt. Columbo. A bulk of events clusters at 3–10 km depth possibly imaging the location of Columbo's magma reservoir and therein the migration of magma and fluids towards the surface. This stresses the active character of this volcano with all its implications for possible future eruptions. The second area with high density of microearthquakes is located NE of Columbo around the island of Anidros possibly consisting of several distinct centers of seismic activity. The activity SE of Amorgos reflects a vertical structure extending between 5 and 15 km depth. The rectangles in the lower part indicate areas investigated by cluster analysis (see text for details).

activity and occurs in a similar way in boxes 3 and 35. It may thus be one typical feature of microseismic activity in the area of investigation. Such activity is likely to be caused by fluids as was observed in different parts of the world (e.g. Kurz et al., 2004). A close relation of swarm-like seismic activity and rising fluids in the Earth's crust was also verified using numerical modeling approaches (e.g. Parotidis et al., 2003). The temporally uniform activity on and around Mykonos (box 13, Fig. 6b) is restricted to magnitudes 2±0.5 to a large extent. This may indicate a constant release of shear stress in this area during our observation period. However, we cannot exclude that this is an artifact of our magnitude threshold of $M=1.8$ and thus $M=2$ may as well reflect the upper boundary of earthquake activity around the island of Mykonos.

4.2. Volcano-related seismicity and cluster activity in the Santorini–Amorgos fault zone

Activity within boxes 37 and 38 is the highest in the area of investigation (Fig. 7C,D and Figs. 5 and 6). The distribution of magnitudes reflects a long-period change of activity within both boxes and clearly indicates the absence of mainshock–aftershock behavior although the magnitude range is high compared to other boxes (which is not an artifact of station distribution). As described earlier, the activity spot ~ 5–10 km NE of Santorini (box 37) represents the today-active Columbo volcanic reef (Dominey-Howes and Minos-Minopoulos, 2004). In fact, boxes 37 and 38 reflect similar long-period changes overprinted on an overall high background activity. Our data suggest a similar activity pattern in both regions, i.e. Columbo and the area around Anidros. However, no volcanic activity has yet been reported for the area around Anidros. To further constrain the distribution of activity along the Santorini–Amorgos zone, we selected all events along its trend of ~ N50°E within a 40 km wide band resulting in a total of 1038 events which is almost half of the entire CYCNET data base. These events are plotted in a depth section in Fig. 8A. The distribution of events along the profile clearly suggests that the activity just NE of Santorini is related to the volcanic activity of Mt. Columbo. A bulk of events clusters at 3–10 km depth possibly imaging the location of Columbo's magma reservoir and therein the migration of magma and fluids towards the surface. This stresses the active character of this volcano with all its implications for possible future eruptions. The second area with high density of micro-earthquakes is located NE of Columbo around the island of Anidros possibly consisting of several distinct centers of seismic activity. Furthermore, we want to put emphasis on the dike-like structure SE of Amorgos extending between 5 and 15 km depth. For further analysis we have to consider that the hypocenters shown in Fig. 8 are absolute locations. The spatio-temporal pattern of seismicity suggests that some areas contain swarm-like activity, possibly with nearly identical waveform which is a commonly observed feature in volcanic regions as shown e.g. for Mt. Etna/Italy (Brancato and Gresta, 2003), Mt. Kilauea/Hawaii (Got et al., 1994) and Volcan de Colima/Mexico (Zobin et al., 2002). Usually such pattern is interpreted as the passive brittle response of the volcanic basement to the intrusion of the eruptive dyke. However, a number of studies (e.g. Hayashi and Morita, 2003; Ukawa and Tsukahara, 1996; Spicak and Horalek, 2001) point out that this might be related to the magma transport in dykes as well. To further investigate this objective for the central HVA and especially for the area NE of Santorini we performed a cluster analysis for distinct regions that are indicated by rectangles in Fig. 8B. For each station and selected area we calculated a separate similarity matrix consisting of all possible event combinations in the selected area. An adaptive time window starting 1 s before the P wave onset and including both the P wave and S wave onset was used for the calculation of the cross correlation coefficient. The data was band pass filtered between 2 and 15 Hz using a Butterworth filter of 3rd order and the time series were normalized. The subdivision of events into different clusters was achieved by a single linkage algorithm which demands that any two members of previously separate clusters must exhibit a correlation coefficient above a certain threshold value in order to merge the two clusters (see Becker et al., this issue, for details). In our analysis a cross correlation coefficient of 0.7 was used as threshold value. As additional constraint it was required that at least two stations meet this cross correlation value for the respective event combination. This approach permits us to perform a relative relocation for the events constituting larger individual clusters to investigate e.g. small-scale migration of hypocenters within distinct clusters. We identified a total of 264 clusters containing more than 1170 events. Though most of the clusters contained only a few events, 20 clusters with more than 10 events were identified which were suitable for relative relocation. The level of clustering is highly variable within the different regions ranging from very low cluster activity in the Ios–Folegandros region to the area between Amorgos and Astypalea in which almost every single event can be associated with a larger cluster.

The activity between Paros and Naxos is of special relevance as it occurs in the otherwise aseismic inner part of the metamorphic core complex as mentioned earlier.

There, 92 out of 132 events can be associated with clusters, mainly duplets and triplets, which separate this activity spot from the generally island-related seismicity that exhibits only minor cluster activity. In Fig. 9 we plotted the results of the cluster analysis for the Columbo–Anidros and Amorgos–Astypalea areas. There, the circles represent the median locations of all events belonging to one cluster and their shading indicates the number of members. Crosses mark single events that belong to a cluster. The Columbo–Anidros area hosts the overall largest cluster activity (118 clusters). Between Amorgos and Astypalea we identified the largest cluster containing 87 events following a 21-member cluster in the same region after 14 months of silence (see also box 31 in Fig. 6). In either of the two regions clusters concentrate in two spots forming sphere-shaped structures below Columbo and Anidros but a more dike-like pattern between Amorgos and Astypalea. To further resolve the hypocentral distribution within the larger clusters we applied a relative relocation technique using the hypoDD code by Waldhauser and Ellsworth (2000) to all clusters with >10 members within the Santorini–Amorgos zone. Apart from the catalogue times which were available from the routine data processing a precise waveform cross correlation was performed to obtain highly accurate relative travel times as input for the relocation scheme. This was done for the P and S onsets separately after resampling the data to 1000 Hz. The differential times

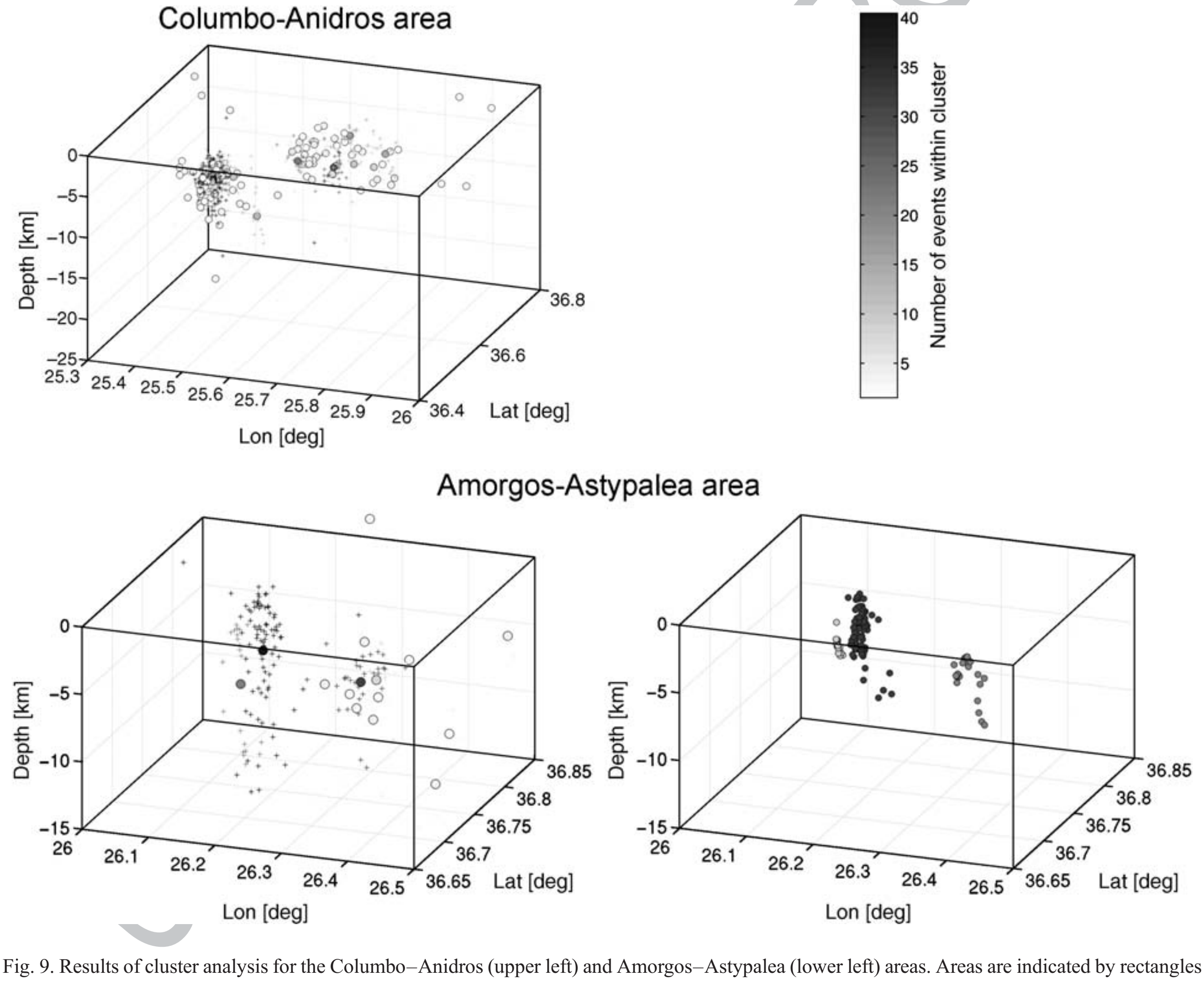

Fig. 9. Results of cluster analysis for the Columbo–Anidros (upper left) and Amorgos–Astypalea (lower left) areas. Areas are indicated by rectangles in Fig. 8. Plotted are the median locations of all events belonging to one cluster indicated by circles (one per cluster). The shading of the circles reflects the number of events contained therein. Crosses indicate events which belong to a cluster. Cluster activity in either area concentrates in two spots forming sphere-shaped structures below Columbo and Anidros but a more dike-like pattern between Amorgos and Astypalea. In addition, we plotted the results of relative relocation for the Amorgos–Astypalea area (lower right) that consists of three main clusters (indicated by the dark grey circles in the lower left). Still the distribution of hypocenters indicates a vertical structure possibly related to the migration of fluids or degassing processes SE of Amorgos.

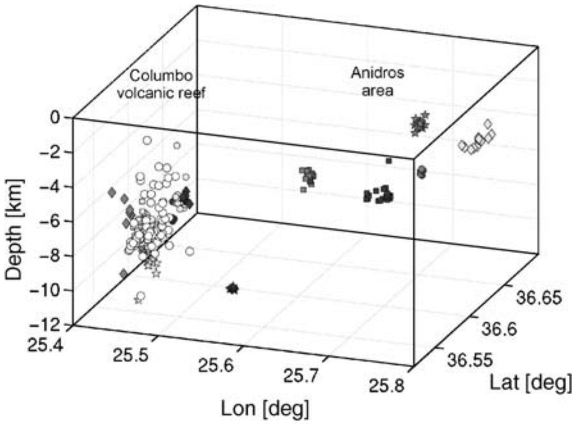

Fig. 10. Results of relative relocation for events contained in the clusters in the Columbo–Anidros area (Fig. 9, upper left). Individual clusters are marked by different symbols. The largest identified cluster contains 162 events and is located below Columbo (white circles). The spatial distribution of relocated hypocenters shows a locally varying pattern. Whereas microearthquakes below Columbo concentrate within one ellipsoidal structure extending between 5 and 8 km depth we identify distinctly separated spots of activity around Anidros. This supports our hypothesis that the Columbo activity might be related to magmatic processes below the volcano possibly representing its magma chamber. In contrast, the activity around Anidros reflects small-scaled activity spots that might represent local pathways of upward migrating fluids within the overall zone of crustal weakness between Santorini and Amorgos or even developing volcanic activity.

obtained from cross correlation were weighted according to their cross correlation coefficients. In Fig. 9 (lower right) we plotted the results of relative relocation for the Amorgos–Astypalea area. Still the distribution of hypocenters indicates a vertical structure possibly related to the migration of fluids or degassing processes SE of Amorgos. However, considering the location error for the vertical direction (up to 3 km for these events) might significantly reduce the vertical extension of this pattern. We thus may only speculate whether these features are related to fluid-extrusion or degassing processes at the seafloor which we suggest to be investigated for this entire region between Santorini and Amorgos in the future. Results for relative relocation of the Columbo–Anidros area are shown in Fig. 10. Distinct clusters in the Columbo–Anidros area are marked by different symbols. The largest identified cluster contains 162 events and is located below Mt. Columbo (white circles). The spatial distribution of events constituting the clusters shows a locally varying pattern. Whereas clusters below Mt. Columbo concentrate within one ellipsoidal structure extending between 5 and 8 km depth we identify distinctly separated spots of activity around Anidros which was not observed from absolute locations. This supports our hypothesis that the Columbo activity might be related to magmatic processes below the volcano possibly representing its magma chamber whereas the activity around Anidros reflects small-scaled activity spots that might represent local pathways of upward migrating fluids within the overall zone of crustal weakness between Santorini and Amorgos or even developing volcanic activity.

4.3. Implications for the regional seismotectonic setting

The distribution of hypocenters contained in the ISC, NOA and also CYCNET catalogues revealed a consistent image of seismicity along the HVA emphasizing that activity is generally higher in the eastern than in the western part. This is of importance as the catalogues cover different magnitude ranges and time intervals as discussed above. Furthermore, the dominant activity along the Santorini–Amorgos zone is highlighted by either catalogue. A similar subdivision along the HVA is observed when considering volcanic activity. In the eastern section, Mt. Columbo is presently the most prominent example being located close to the Santorini complex with its devastating eruptions in historic times. Apart, also the Nisyros volcano showed high and even increasing activity (Papadopoulos et al., 1998; Sachpazi et al., 2002). In contrast, decreasing volcanic activity is observed in the western HVA at Milos and Aegina (e.g. Rinaldi and Campos Vinuti, 2003). Both observations require a transitional zone or even a sharp structural boundary in between. In Fig. 11 we plotted the catalogue of historic seismicity that was compiled by Papazachos et al. (2000) for the central HVA. The distribution of hypocenters covers ~ 2000 years for the larger magnitudes and supports our hypothesis of a subdivided volcanic arc giving further evidence that the boundary in between both parts of the HVA is represented by a zone of crustal weakness in the Santorini–Amorgos area. Interestingly, this area also faced the two largest earthquakes in the entire Aegean region during the last century. Both events occurred within only 13 min in July 1956 ($M_s = 7.4$ and 7.2) and where followed by at least 20 aftershocks of $M > 4$ (Papadopoulos and Pavlides, 1992). Furthermore, the two mainshocks caused a tsunami with regional impact reaching water-wave amplitudes > 6 m (Ambraseys, 1960; Perissoratis and Papadopoulos, 1999). Papadopoulos and Pavlides (1992) analyzed the 1956 seismic sequence including field mapping from Amorgos and concluded on a NW–SE-trending main extensional stress for the Santorini–Amorgos fault region which is supported by the fault mechanism of the 1956 mainshock (see discussion in their paper). The NW–SE extensional character of this area is confirmed by Hatzfeld et al. (1993) who propose a normal faulting

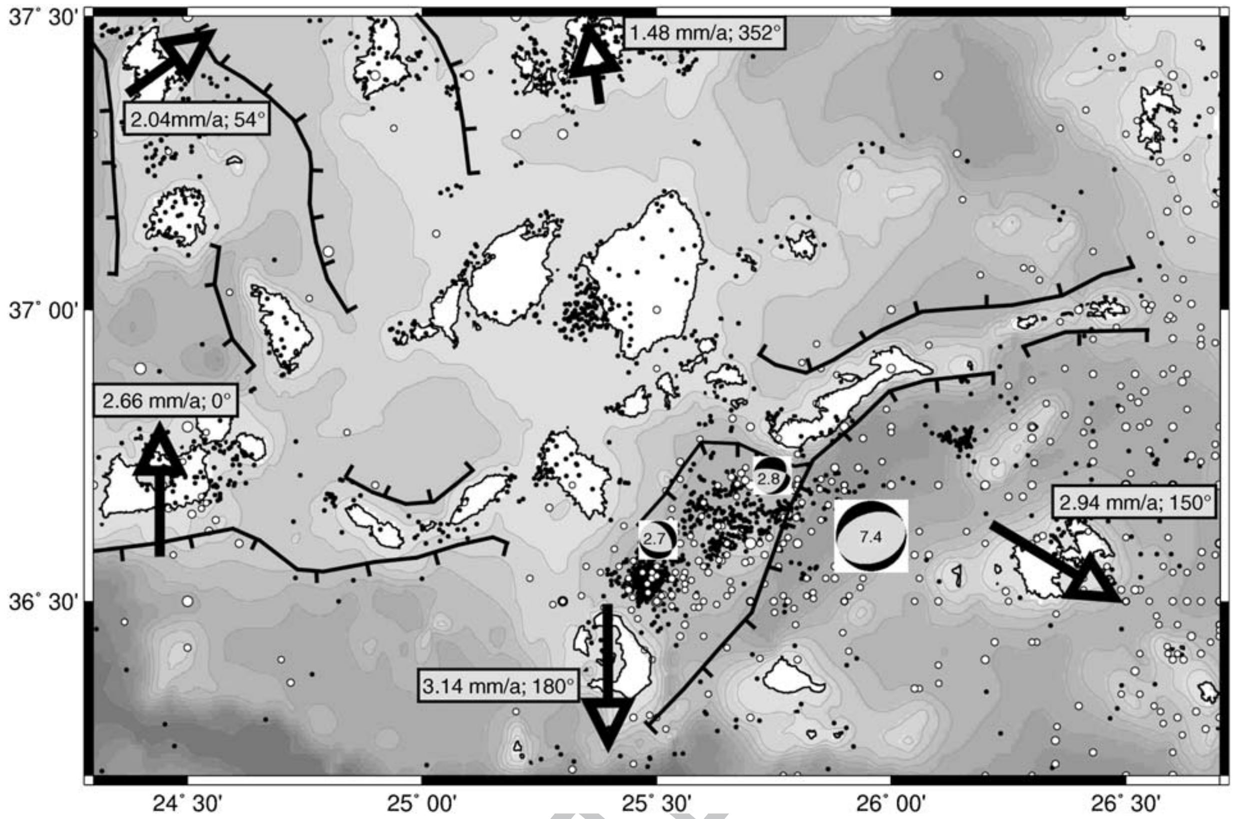

Fig. 11. Present seismotectonic setting for the central Hellenic Volcanic Arc. Small black dots are hypocenters recorded by CYCNET and large white dots are hypocenters of the historical seismicity catalogue (Papazachos et al., 2000). Black lines indicate major fault structures of the area (simplified after Gautier and Brun, 1994; Tsapanos et al., 1994). Arrows show the GPS-derived horizontal velocity field after Mc Clusky et al. (2000) in a central Hellenic Volcanic Arc reference frame (see Table 2 and text for details). Fault plane solutions are taken from Hatzfeld et al. (1993, events of 1988 with M=2.7 and 2.8) and from Papadopoulos and Pavlides, 1992, (1956 mainshock with M=7.4). Results uniformly stress that the Santorini–Amorgos zone marks a major structural boundary in a right-lateral transtensional regime that subdivides the Hellenic Volcanic Arc into a seismically and volcanically quiet western and an active eastern part.

regime with roughly NS trending T axes based on two focal mechanisms that are plotted in Fig. 11.

CYCNET earthquake hypocenters are also plotted in Fig. 11 (black dots). Although both catalogues cover widely different time and magnitude intervals, the Santorini–Amorgos zone is a common prominent feature in either one indicating that this region represents a major structural boundary between the eastern and western parts of the HVA. To further evaluate the present setting of this zone we implement information on the GPS-derived horizontal velocity field of this region. The most comprehensive study for the Aegean–Anatolian region was presented by Mc Clusky et al. (2000) refining earlier observations of relative plate motion for this region. They report on an average 3.2 cm/a SW-ward movement of the south Aegean with little internal deformation in the order of several mm/a only. In their Fig. 8 they plotted the GPS-horizontal velocity field in a south Aegean reference frame indicating a SE-ward migrating eastern part of the Hellenic subduction zone with respect to the western part. This is also consistent with results obtained by Bohnhoff et al. (~~in press~~) who analyzed the deformation and stress fields along the Hellenic arc based on focal mechanisms.

Table 2
GPS-horizontal velocity field in the central HVA based on data from Mc Clusky et al., 2000

Site	Island	In Eurasian frame		In central HVA frame		
		N	E	N	E	Trend
		[mm/a]	[mm/a]	[mm/a]	[mm/a]	[N°E]
KYNS	Kythnos	−26.20	−17.60	1.66	1.20	54
MILO	Milos	−25.20	−16.40	2.66	0.00	0
MKN2	Mykonos	−26.40	−16.60	1.46	−0.20	352
ASTP	Astypalea	−30.50	−14.90	−2.54	1.48	150
THIR	Santorini	−31.00	−16.40	−3.14	0.00	180
Average central HVA		−27.86	−16.38			

See text for details.

To further resolve the GPS observations by Mc Clusky et al. (2000) we convert their data into a central HVA reference frame by averaging the five available data points that are located on the islands of Kythnos, Milos, Mykonos, Santorini (Thira) and Astypalea (Table 2). The resulting vectors reach ~ 5 mm/a of internal deformation within the central HVA with a systematically varying trend (Fig. 11) and confirm a subdivision of the HVA in a western and eastern part with the Santorini–Amorgos zone representing the internal transitional zone. Furthermore, these results support our conclusion of a right-lateral transtensional character of the central HVA and the direction of extension being NW–SE.

To constrain the above described model we relate our findings to structural maps of the south Aegean region (see e.g. Tsapanos et al., 1994; Gautier and Brun, 1994, and references therein). They consistently show two types of major faulting directions. Earlier E–W trending normal faults—that today form the horst structures that also host significant microseismic activity as presented in this study—were later overprinted by SW–NE trending normal faults. These faults are presently active as documented by CYCNET data (see also discussion in Perissoratis, 1995). Selected major branches of these fault systems (E–W, SW–NE) are plotted in Fig. 11 and allow to identify that a large portion of these faults is located in the presently active Santorini–Amorgos zone that represents a major boundary within the HVA.

We conclude that the Santorini–Amorgos area is a zone of crustal weakness in an overall right-lateral transtensional regime. It represents a major structural boundary in the HVA which is required by independent observations from different disciplines. This results in a subdivision of the volcanic arc. The western part is characterized by considerably lower seismic activity (as also identified by Papanikolaou, 1981, based on a much sparser hypocenter catalogue) and decreasing volcanic activity (Aegina, Milos) within the last 40 ka. In contrast, the eastern HVA is characterized by generally higher seismic and volcanic activity focused on the Santorini–Amorgos area and the Nisyros area as central part of the Dodecanese island group.

5. Conclusions

We presented results from a low magnitude-detection threshold seismic monitoring ~~experiment~~ in the central Hellenic Volcanic Arc (HVA). Strong seismic activity that is clustered in space and time was identified in regions considered to be aseismic from catalogs containing earthquakes of $M>3$. Microseismic activity is linked to the occurrence of islands that represent horst structures or concentrated in the Santorini–Amorgos zone that also hosted the two largest earthquakes in the entire south Aegean region within the last century. We identified four different types of spatio-temporal behavior of microseismic activity. Cluster analysis revealed that more than fifty percent of events can be associated with cluster activity and relative relocation partly allows resolving their internal structure. The most prominent feature is the submarine Columbo volcano NE of Santorini with dominant activity concentrated in the uppermost 5–8 km. This activity is interpreted to be linked to the accumulation of magma below the volcano. Distinct activity spots around Anidros further to the NE are likely locations for future volcanic activity in this zone of crustal weakness or may indicate fluid pathways.

The Santorini–Amorgos zone developed in a right-lateral transtensional regime and is interpreted to mark a major structural boundary of the volcanic arc subdividing the HVA into a seismically and volcanically quiet western and an active eastern part. This model is supported by the GPS-derived horizontal velocity field, the distribution of historical earthquakes and by the occurrence of major faults in this region. The results emphasize that appropriate temporary seismic networks are an adequate tool to develop comprehensive regional seismotectonic models in selected regions.

Acknowledgements

We acknowledge constructive reviews by D. Hatzfeld and T. Wright that helped to improve the manuscript. We are grateful to J. Baskoutas, B. Klotz, L. Kühne and G. Michaletos for their support during installation and maintenance of the seismic stations on the islands under partly difficult conditions. This program was funded by the German Research Foundation (DFG) within the Collaborative Research Center 526 entitled 'Rheology of the Earth — from the Upper Crust to the Subduction Zone'. We thank the GeoForschungsZentrum Potsdam for supplying seismic acquisition systems from the Geophysical Instrument Pool.

References

Ambraseys, N.N., 1960. The seismic sea wave of July 9, 1956 in the Greek Archipelago. J. Geophys. Res. 65, 1257–1265.

Avigad, D., Garfunkel, Z., 1989. Low-angle faults above and below a blueschist belt—Tinos Island, Cyclades, Greece. Terra Nova 1, 182–187.

Avigad, D., Ziv, A., Garfunkel, Z., 2001. Ductile and brittle shortening, extension–parallel folds and maintenance of crustal thickness in the central Aegean (Cyclades, Greece). Tectonics 20/2, 277–287.

Becker, D., Meier, T., Rische, M., Bohnhoff, M., Harjes, H.-P., 2005. Spatio-temporal microseismicity clustering in the Cretan region, this issue.

Bohnhoff, M., Harjes, H.-P., Meier, T., 2005. Deformation and stress regimes in the Hellenic subduction zone from focal mechanisms. J. Seismology, ~~in press~~.

Bohnhoff, M., Rische, M., Meier, T., Endrun, B., Harjes, H.-P., Stavrakakis, G., 2004. A temporary seismic network on the Cyclades (Aegean Sea, Greece). Seismol. Res. Lett. 75/3, 352–357.

Brancato, A., Gresta, S., 2003. High-precision relocation of microearthquakes at Mt. Etna (1991–1993 eruption onset): a tool for better understanding the volcano seismicity. J. Volcanol. Geotherm. Res. 124, 219–239.

Brönner, M., 2003. Untersuchungen des Krustenaufbaus entlang des Mediterranen Rückens abgeleitet aus geophysikalischen Messungen, PhD thesis. Faculty of Geosciences, Hamburg University (in German).

Dominey-Howes, D., 2004. A re-analysis of the Late Bronze Age eruption and tsunami of Santorini, Greece, and the implications for the volcano–tsunami hazard. J. Volcanol. Geotherm. Res. 130, 107–132.

Dominey-Howes, D., Minos-Minopoulos, D., 2004. Perceptions of hazard and risk on Santorini. J. Volcanol. Geotherm. Res. 137, 285–310.

Druitt, T.H., Edwards, L., Mellors, R.M., Pyle, D.M., Sparks, R.S.J., Lamphere, M., Davies, M., Barreiro, B., 1999. Santorini volcano. Memoirs, vol. 19. Geological Society, London. 165 pp.

Earth Data Ltd., 2002. Instruction Manual for PR6-24 Seismic Datalogger, EDM021 (2). Southampton/U.K., 53 pages.

Endrun, B., Ceranna, L., Meier, T., Bohnhoff, M., Harjes, H.-P., 2005. Modeling the influence of Moho topography on receiver functions: a case study from the central Hellenic subduction zone. Geophys. Res. Lett. 32, L12311, doi:10.1029/2005GL023066.

Engdahl, E.R., Van Der Hilst, R., Buland, R., 1998. Global teleseismic earthquake relocation with improved travel times and procedures for depth determination. Bull. Seismol. Soc. Am. 88, 722–743.

Friedrich, W., 2000. Fire in the Sea. The Santorini Volcano: Natural History and the Legend of Atlantis. Cambridge University Press. 257 pp.

Galanopoulos, A.G., 1963. On mapping of seismic activity in Greece. Ann. Geofis. 16, 37–100.

Gautier, P., Brun, J.P., 1994. Crustal-scale geometry and kinematics of late-orogenic extension in the central Aegean (Cyclades and Evvia Island). Tectonophysics 238, 399–424.

Gautier, P., Brun, J.P., Jolivet, L., 1993. Structure and kinematics of Upper Cenozoic extensional detachment on Naxos and Paros (Cyclades islands, Greece). Tectonics 12, 1180–1194.

Gautier, P., Brun, J.P., Moriceau, R., Sokoutis, D., Martinod, J., Jolivet, L., 1999. Timing, kinematics and cause of Aegean extension: a scenario based on comparison with simple analogue experiments. Tectonophysics 315, 31–72.

Got, L., Frechet, M.J., Klein, F.W., 1994. Deep fault plane geometry inferred from multiplet relative location beneath the south flank of Kilauea. J. Geophys. Res. 99, 15375–15386.

Hanka, W., Kind, R., 1994. The GEOFON program. Ann. Geofis. 37, 1060–1065.

Hatzfeld, D., Besnard, M., Makropoulos, K., 1993. Microeartquake seismicity and fault-plane solutions in the southern Aegean and its geodynamic implications. Geophys. J. Int. 115, 799–818.

Hayashi, H., Morita, Y., 2003. An image of a magma intrusion process inferred from precise hypocentral migrations of the earthquake swarm east of the Izu Peninsula. Geophys. J. Int. 153, 159–174.

Jackson, J., 1994. Active tectonics of the Aegean region. Annu. Rev. Earth Planet. Sci. 22, 239–271.

Jackson, J., McKenzie, D.P., 1988. The relationship between plate motion and seismic moment tensors, and the rates of active deformation in the Mediterranean and Middle East. Geophys. J. 93, 45–73.

Keller, J., Rehren, Th., Stadlbauer, E., 1990. Explosive volcanism in the Hellenic arc: a summary and review. Proceedings of the third International Congress, Thera and the Aegean World III, vol. 2, pp. 13–26.

Kurz, J.H., Jahr, T., Jentzsch, G., 2004. Earthquake swarm examples and a look at the generation mechanism of the Vogtland/Bohemia earthquake swarm. Phys. Earth Planet. Inter. 142, 75–88.

Lee, W.H.K., Lahr, J.C., 1972. HYPO71: a computer program for determining hypocenter magnitude, and first motion pattern of local earthquakes. U.S. Geological Survey Open-File Report.

Lee, W.H.K., Lahr, J.C., 1975. HYPO71 (revised): a computer program for determining hypocenter, magnitude, and first motion pattern of local earthquakes. U.S. Geological Survey Open-File Report.

Le Pichon, X., Angelier, J., 1979. The Hellenic arc and trench system: a key to the neotectonic evolution of the Eastern Mediterranean area. Tectonophysics 60, 1–42.

Le Pichon, X., Chamot-Rooke, N., Lallemant, S., 1995. Geodetic determination of the kinematics of central Greece with respect to Europe: implications for eastern Mediterranean tectonics. J. Geophys. Res. 100, 12675–12690.

Lister, G.S., Banga, G., Feenstra, A., 1984. Metamorphic core complexes of Cordilleran type in the Cyclades, Aegean Sea, Greece. Geology 12, 221–225.

Makris, J., Chonia, T., 1999. Active and passive seismic studies of Nisyros Volcano — East Aegean Sea. In: Jacob, A.W.B., Bean, C.J., Jacob, S.T.F. (Eds.), Proceedings of the 1999 CCSS Workshop, Communications of the Dublin Institute for Advanced StudiesSeries D, Geophysical Bulletin, vol. 49, pp. 9–12.

Makropoulos, K.C., Burton, P.W., 1981. A catalogue of seismicity in Greece and adjacent areas. Geophys. J.R. Astron. Soc. 65, 741–762.

Mc Kenzie, D.P., 1970. Plate tectonics of the Mediterranean region. Nature 226, 239–243.

Mc Clusky, S., et al., 2000. Global Positioning System constraints on plate kinematics and dynamics in the eastern Mediterranean and Caucasus. J. Geophys. Res. 105, 5695–5719.

Meier, T., Dietrich, K., Stöckhert, B., Harjes, H.-P., 2004. One-dimensional models of shear wave velocity for the eastern Mediterranean obtained from the inversion of Rayleigh wave phase velocities and tectonic implications. Geophys. J. Int. 156, 45–58.

Ochmann, N., Hollnack, D., Wohlenberg, J., 1989. Seismological exploration of the Milos geothermal reservoir, Greece. Geothermics 18 (4), 563–577.

Panagiotopoulos, D.G., Stavrakakis, G., Makropoulos, K., Papanstasiou, D., Papazachos, C., Savvidis, A., Karagianni, A., 1996. Seismic monitoring at the Santorini volcano, the European laboratory volcanoes. Proceedings of the Second Workshop Santorini, Greece, pp. 311–324.

Papadopoulos, G.A., Pavlides, S.B., 1992. The large 1956 earthquake in the South Aegean: macroseismic field configuration, faulting and neotectonics of Amorgos island. Earth Planet. Sci. Lett. 113, 383–396.

Papadopoulos, G.A., Kondopoulou, D.P., Leventakis, G.A., Pavlides, S.B., 1986. Seismotectonics of the Aegean region. Tectonophysics 124, 67–84.

Papadopoulos, G., Sachpazi, M., Panopoulou, G., Stavrakakis, G., 1998. The volcanoseismic crisis of 1996–1997 in Nisyros, SE Aegean Sea, Greece. Terra Nova 10, 151–154.

Papazachos, B.C., 1973. Distribution of seismic foci in the Mediterranean and surrounding area and its tectonic implications. Geophys. J.R. Astron. Soc. 33, 421–430.

Papazachos, B.C., Karakostas, V.G., Papazachos, C.B., Scordilis, E.M., 2000. The geometry of the Wadati–Benioff zone and lithospheric kinematics in the Hellenic arc. Tectonophysics 319, 275–300.

Parotidis, M., Rothert, E., Shapiro, S.A., 2003. Pore-pressure diffusion: a possible triggering mechanism for the earthquake swarms 2000 in Vogtland/NW-Bohemia, central Europe. Geophys. Res. Lett. 30, doi:10.1029/2003GL018110.

Perissoratis, C., 1995. The Santorini volcanic complex and its relation to the stratigraphy and structure of the Aegean arc, Greece. Mar. Geol. 128, 37–58.

Perissoratis, C., Papadopoulos, G., 1999. Sediment instability and slumping in the southern Aegean Sea and the case history of the 1956 tsunami. Mar. Geol. 161, 287–305.

Rinaldi, M., Campos Vinuti, M., 2003. The submarine eruption of the Bombarda volcano, Milos island, Cyclades, Greece. Bull. Volcanol. 65, 282–293.

Sachpazi, M., Kontoes, Ch., Voulgaris, N., Laigle, M., Vougioukalakis, G., Sikioti, O., Stavrakakis, G., Baskoutas, J., Kalogeras, J., Lepine, J.Cl., 2002. Seismological and SAR signature of unrest at Nisyros caldera, Greece. J. Volcanol. Geotherm. Res. 116, 19–33.

Spicak, A., Horalek, J., 2001. Possible role of fluids in the process of earthquake swarm generation in the West Bohemia/Vogtland seismoactive region. Tectonophysics 336, 151–161.

Tirel, C., Gueydan, F., Tiberi, C., Brun, J.P., 2004. Aegean crustal thickness inferred from gravity inversion. Geodynamical implications. Earth Planet. Sci. Lett. 228, 267–280.

Trotet, F., Jolivet, L., Vidal, O., 2001. Tectono-metamorphic evolution of Syros and Sifnos islands (Cyclades, Greece). Tectonophysics 338, 179–206.

Tsapanos, T.M., Galanopoulos, D., Burton, P.W., 1994. Seismicity in the Hellenic Volcanic Arc: relation between seismic parameters and the geophysical fields in the region. Geophys. J. Int. 117, 677–694.

Ukawa, M., Tsukahara, H., 1996. Earthquake swarms and dike intrusions off the east coast of Izu Peninsula, central Japan. Tectonophysics 253, 285–303.

Vougioukalakis, G., et al., 1994. The submarine volcanic centre of Kolumbo, Santorini, Greece. Bull. Geol. Soc. G. B. XXX/3, 351–360.

Walcott, C.R., White, S.H., 1998. Constraints on the kinematics of post-orogenic extension imposed by stretching lineations in the Aegean region. Tectonophysics 298, 155–175.

Waldhauser, F., Ellsworth, W.L., 2000. A double difference earthquake location algorithm: method and application to the northern Hayward fault. Bull. Seismol. Soc. Am. 90, 1353–1368.

Zobin, V.M., Gonzales Amezcua, M., Reyes Davila, G.A., Dominguez, T., Chacon, J.C., Chavez Alvarez, J.M., 2002. Comparative characteristics of the 1997–1998 seismic swarms preceding the November 1998 eruption of Volcan de Colima, Mexico. J. Volcanol. Geotherm. Res. 117, 47–60.